WATER RESOURCES RESEARCH, VOL. 31, NO. 8, PAGES 2035–2045, AUGUST 1995

Modeling transport of multiple organic compounds: Segregated transport-sorption/solubilization numerical technique

Zafar Adeel and Richard G. Luthy
Department of Civil and Environmental Engineering, Carnegie Mellon University, Pittsburgh, Pennsylvania

David A. Edwards
H & A of New York, Rochester

Abstract. The transport of multiple organic contaminants in the subsurface may be affected by their mutual interactions. Conventional modeling approaches cannot simulate the transport of multiple organic species whose sorption and/or solubilization is interdependent. This paper describes a numerical modeling approach for characterizing interactive solute sorption and solubilization reactions coupled with one-dimensional advective–dispersive transport in porous media. This numerical approach, referred to as segregated transport-sorption/solubilization (STSS), allows for interphase mass transfer at each time step after solute advection and dispersion have occurred. The overall capabilities of the STSS technique include modeling equilibrium or nonequilibrium transport of individual and multiple solutes with linear or nonlinear sorption isotherms. Application of this modeling approach is illustrated for the transport of a conservative tracer, a surfactant, a hydrophobic organic compound (HOC), and a polychlorinated biphenyl (PCB) mixture. The coupling of sorption modules for phenanthrene and surfactant is used to reasonably describe surfactant-enhanced flushing of sorbed phenanthrene from a sand column.

Introduction

Predictive models are used to evaluate contaminant transport in subsurface media and groundwater. A potential difficulty in applying existing models to situations involving organic contaminants is that these contamination scenarios rarely comprise pure organic compounds. For example, organic contaminants of concern are often associated with other organic compounds that may be present as a separate nonaqueous liquid mixture in the subsurface [*Mackay and Cherry*, 1989; *Abdul and Gibson*, 1991; *Feenstra*, 1992]. The transport of individual components from an organic mixture can be dependent on interactions among the mixture components as well as other organic compounds in the subsurface. Examples of component interactions that may affect organic compound transport include those between organic compounds and other organic-phase matter including humic cosolutes [*Wershaw*, 1986; *Magee et al.*, 1991], organic cosolvents [*Nkeddi-Kizza et al.*, 1987], surfactant micelles [*Valsaraj and Thibodeaux*, 1989], and surfactant cosorbates [*Lee et al.*, 1989; *Holsen et al.*, 1991]. In order to be concise, the discussion in this paper considers only cases where contaminants are present in a dissolved, solubilized, or sorbed phase.

In general, contaminant transport problems for multiple organic compounds can be categorized according to the extent of interaction and the nature of sorption of the individual solutes. The interaction of multiple solutes may generally be ignored when the solutes are present at low aqueous concentrations, because solute–water interactions dominate behavior of the dissolved species, and solute–solute interactions are not significant due to a high degree of dilution [*Mackay et al.*, 1991]. However, in the case of micellar surfactant solution flushing of hydrophobic organic compounds (HOCs), surfactant–solute interactions dominate over water–solute interactions because of the strong tendency of HOCs to partition into surfactant micelles. The complicated nature of sorption of HOCs and nonionic surfactant onto aquifer materials has been studied previously [*Lee et al.*, 1989; *Pennell et al.*, 1993; *Edwards et al.*, 1994; *Adeel and Luthy*, 1995].

A generalized modeling approach should be capable of incorporating both local equilibrium and nonequilibrium sorption phenomena for organic compound transport. Also, the most general form of a numerical transport model should provide stable and accurate predictions while accommodating a range of flow velocities and hydrodynamic dispersivities. In relation to the general problem of transport of sorbing organic contaminants in subsurface systems, the following types of modeling scenarios may be encountered: Type 1, equilibrium transport of a single solute; Type 2, nonequilibrium transport of a single solute; Type 3, equilibrium transport of multiple, noninteractive solute species; Type 4, nonequilibrium transport of multiple, noninteractive solute species; Type 5, equilibrium transport of multiple, interactive solute species; and Type 6, nonequilibrium transport of multiple, interactive solute species.

Mathematical Modeling Approach

This paper presents a segregated transport-sorption/solubilization (STSS) numerical technique that can accommo-

Paper number 95WR01331.
0043-1397/95/95WR-01331$05.00

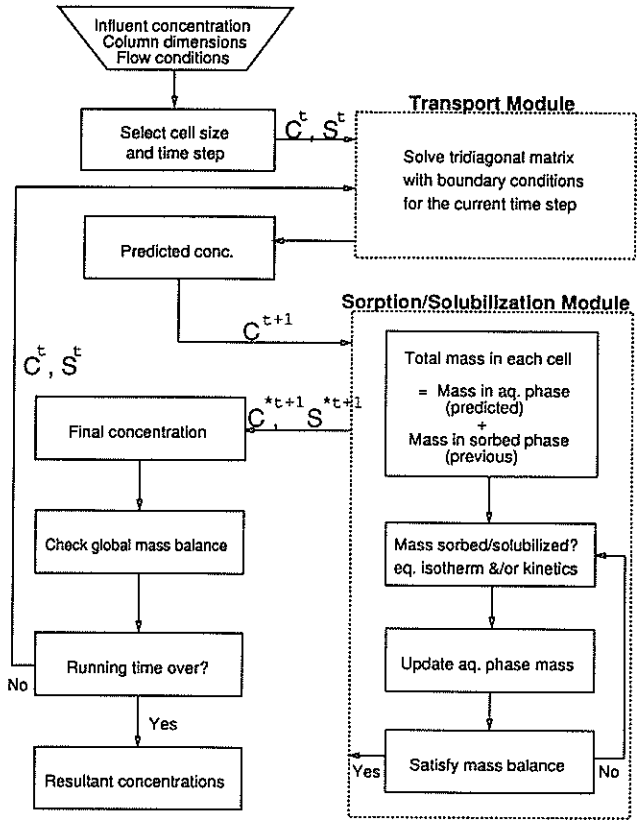

Figure 1. A schematic outline of different components of the STSS technique.

date multiple component, one-dimensional interactive solute transport phenomena. In principle, this mathematical technique can be extended to multiple dimensions. The STSS approach divides the flow domain into discrete cells and considers the phase transformation phenomena independently of the transport mechanism during each time step in each cell. Dissolved or solubilized solute mass is moved at the beginning of a given time step by considering transport by advection and dispersion. This is followed by interphase mass transfer in each cell during that time step. The time dependency of the interphase mass transfer process can be specified, or alternatively, local equilibrium can be assumed. A number of solutes and/or sorbents may be included.

The modeling process is outlined schematically in Figure 1; individual components of the model are discussed more fully in subsequent sections. A numerical technique is used to estimate unknown parameters associated with nonequilibrium-sorption/transport phenomena. Treating the mathematics of sorption and/or solubilization equations independently at each time step from the advection–dispersion equations has several benefits over accounting for multiple processes in a single equation. In the STSS technique the relationship among the concentration of a solute in different phases can be varied at each time step and at different locations. Such flexibility allows for explicit consideration of the spatial and temporal variation in the interaction of multiple solutes when their sorption and solubilization rates are distinctly different. In order to demonstrate its applicability to the six organic contaminant transport scenarios described previously, the STSS technique is applied to several situations to predict experimental data or to simulate hypothetical cases.

The numerical modeling approach of segregating transport and transformation phenomena has been used successfully in air pollutant transport models [*McRae et al.*, 1982]. This technique has also been used with some success in groundwater transport models for mineral dissolution and ion exchange of different solutes [*Grove and Wood*, 1979; *Schulz and Reardon*, 1983; *Cederberg et al.*, 1992; *Šimůnek and Suarez*, 1994]. Some stochastic models for transport of solutes through groundwater also utilize a similar modeling approach [*Prickett et al.*, 1981]. Apparently, this technique has not been applied for modeling the transport of organic contaminants in groundwater.

After briefly discussing the conventional approaches to modeling transport of organic solutes, this paper will present the STSS mathematical formulation and apply this technique to several different simulations to demonstrate the versatility of the approach. One-dimensional transport is simulated for the following cases:

1. Transport of a conservative tracer through a laboratory-scale column. This is a special case of Type 1 transport, where no sorption occurs.
2. Transport of phenanthrene, an HOC, in a laboratory-scale column. Type 1 and Type 2 transport are simulated.
3. Transport of Triton X-100, a nonionic surfactant, in a laboratory-scale column. This is another example of Type 2 transport.
4. Coupled transport of phenanthrene and Triton X-100. Equilibrium sorption for both the solutes is assumed in order to demonstrate Type 5 transport.
5. Coupled transport of phenanthrene and Triton X-100. The model predictions using nonequilibrium sorption modules are compared against experimental data in this example of Type 6 transport.
6. Transport of different PCB congeners from a contaminated source region in an aquifer. Linear, nonequilibrium sorption modules are used for each PCB congener in this simulation (Type 4).

Conventional Solute Transport Model

The conventional approach to modeling the transport of an organic solute through a porous medium has been to employ an advection–dispersion equation formulated to account for reactions such as sorption, biological degradation, and chemical decomposition. A number of analytical and numerical techniques for solving these equations under a variety of flow conformations have been presented in the literature [*Enfield et al.*, 1982; *Grove and Stollenwerk*, 1984; *van Genuchten and Alves*, 1982; *Molz et al.*, 1986; *Srinivasan and Mercer*, 1988; *Brusseau*, 1992]. The one-dimensional transport of a single, linearly sorbing organic solute with local equilibrium under steady flow conditions is mathematically described by [*van Genuchten and Alves*, 1982]

$$\frac{\partial C}{\partial t} + \frac{\rho}{\theta}\frac{\partial S}{\partial t} = D\frac{\partial^2 C}{\partial x^2} - v\frac{\partial C}{\partial x} \tag{1}$$

where C is the flux-averaged concentration of the solute in aqueous phase (ML^{-3}), S is mass of solute sorbed per unit weight of the solid phase (MM^{-1}), x is the distance along the direction of flow (L), D is the hydrodynamic dispersion coefficient (L^2T^{-1}), t is time (T), v is the average pore water (seepage) velocity (LT^{-1}), ρ is the dry bulk density (ML^{-3}), and θ is the fractional pore volume in the porous medium

(L^3L^{-3}). In order to solve (1) analytically or numerically using conventional techniques, the sorbed concentration S must be defined in terms of aqueous concentration (C). An analytical solution has not been developed for (1) that can characterize cases for which temporal and spatial variation of the relationship between S and C affect the partitioning process, that is, Types 5 and 6 transport for interacting cosolutes and/or cosorbates.

Transport Module

As a first step in the STSS technique, the solute in a given cell is advected and dispersed through the porous medium, with the solute being considered nonreactive. The one-dimensional form of the advection–dispersion equation for transport of nonreactive solutes under steady, uniform flow when $\partial S/\partial t$ is zero follows from (1):

$$\frac{\partial C}{\partial t} = D\frac{\partial^2 C}{\partial x^2} - v\frac{\partial C}{\partial x} \tag{2}$$

with all variables the same as in (1). Here (2) can be solved analytically for a number of different boundary and flow conditions [*van Genuchten and Alves*, 1982]. In order to be consistent with the finite differencing approach employed for solving the differential equations controlling the sorption/solubilization processes, the Crank–Nicholson approach is used. A partially implicit technique, such as the Crank–Nicholson approach, is required to obtain an algorithm sufficiently robust and stable to accommodate various flow conditions [*Grove and Stollenwerk*, 1984]. The flow domain is divided into a number of small cells of length (Δx), and the length of each time step is correlated to cell length and flow velocity ($\Delta t = \Delta x/v$). The solute residence time (Δt) signifies the time taken by a plug of solute to travel the length of the imaginary cell. A flux-type (Cauchy type) inlet boundary is used, which conserves mass in semifinite columns as well as in finite columns. A Dirichlet-type boundary is used at the outlet, as it has been shown to reasonably describe the outlet boundary in cases where the Peclet number (ratio of advective flux to dispersive flux) for the column is greater than five [*van Genuchten and Parker*, 1984].

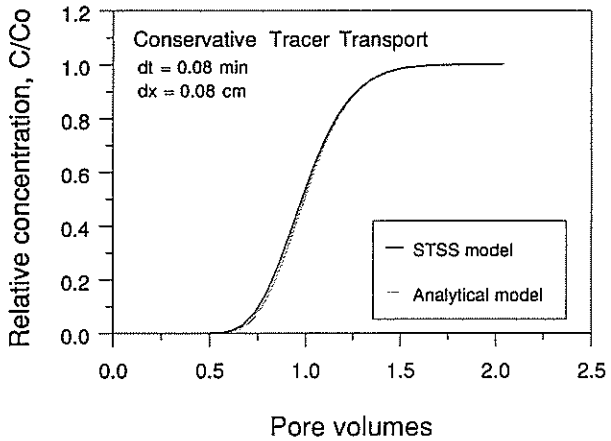

Figure 2. A comparison of the predictions from the numerical STSS approach and the analytical solution by *Parker and van Genuchten* [1984]. Simulated for transport of a conservative tracer through 2.20-cm ID, 7.53-cm-long column with average pore water velocity of 3.78 cm/min, dispersivity of 0.15 cm, and porosity of 0.34.

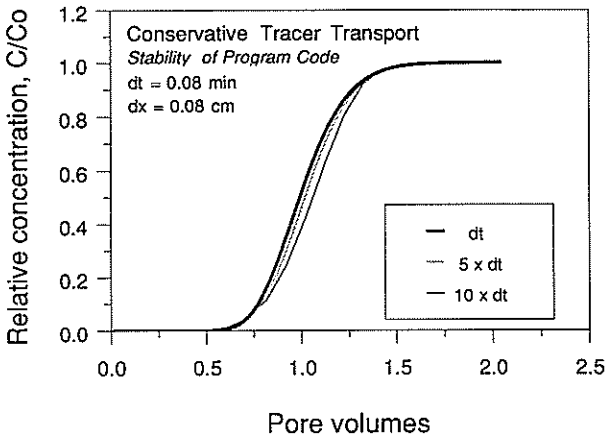

Figure 3. A comparison of the transport module outputs of the STSS model at different time steps. Simulated for flow of a conservative tracer through the column described in Figure 2.

The transport module of the STSS model is validated by comparing the model prediction for one-dimensional column transport of a conservative solute to that of a conventional model [*Parker and van Genuchten*, 1984]; the results are shown in Figure 2. Predictions from the conventional and the numerical STSS techniques are virtually indistinguishable. The stability of the numerical computer code can be demonstrated by executing the program at time step sizes greater than those determined by $\Delta t = \Delta x/v$, as shown in Figure 3. The time step was increased to 5 and 10 times the computed cell residence time and it was observed that even relatively large time steps provide reasonably reliable results.

Sorption/Solubilization Modules

The STSS technique is sufficiently flexible to incorporate various types of sorption or phase transfer reactions. In this section, the discussion has been restricted to local equilibrium and nonequilibrium sorption/solubilization models.

Sorption with Local Equilibrium

Equilibrium, noninteractive sorption. A generalized form for describing the equilibrium relationship between the sorbed-phase concentration S and the aqueous-phase concentration C of a solute is

$$S = g(C) \tag{3}$$

where $g(C)$ is a function that characterizes a linear or a nonlinear sorption isotherm. During each time step, the transport module provides an aqueous-phase concentration (C_i^{t+1}) for time ($t + 1$) in a cell (i). The mass sorbed per unit weight of the solid phase, as computed from the previous time step or initial conditions (S_i^t) is also known. A mass conservation computation over the total cell volume is performed according to (3). Evaluating the equilibrated concentrations C_i^{*t+1} and S_i^{*t+1} require simultaneous, noniterative solution of the following linear equations:

$$S_i^{*t+1} = g(C_i^{*t+1}) \tag{4}$$

$$M_i^{t+1} = \theta C_i^{*t+i} + \rho S_i^{*t+1} \tag{5}$$

The concentrations C_i^{*t+1} and S_i^{*t+1} are then used as initial concentrations for the next time step of the transport model.

Equilibrium, interactive sorption. A good example of interacting species is surfactant-enhanced solubilization and transport of HOC compounds in the subsurface. The distribution of an HOC between bulk aqueous and solid phases can be affected strongly by the presence of a nonionic surfactant at concentrations above the critical micelle concentration (CMC) [*Abdul et al.*, 1990; *Edwards et al.*, 1994]. Surfactant micelles in an aqueous phase can greatly enhance the apparent solubility of an HOC as a result of partitioning of HOCs into the surfactant micelles (collectively referred to as a micellar pseudophase). On the other hand, sorbed surfactant on solid media can enhance sorption of the HOC. However, at high, supra-CMC surfactant concentrations, solubility enhancement dominates the overall partitioning behavior of an HOC.

A measure of the enhanced solubilization of an HOC is the decrease in the value of its apparent solid/water partition coefficient (K_d). For a system of Lincoln fine sand, Triton X-100, and phenanthrene, an inverse relationship exists between K_d and the bulk-aqueous phase surfactant concentration (C_s). Data presented by *Edwards et al.* [1994] for this system show that only after the aqueous surfactant concentration increases beyond 0.78 mM, termed C_{int}, is the enhanced solubilization in the micellar pseudophase large enough to overcome the increased phenanthrene sorption due to the sorbed surfactant molecules, for which

$$1/K_d = 159000C_s - 125 \tag{6}$$

This relationship means that the isotherm expression given by (3) can be modified to account for the effect of Triton X-100 nonionic surfactant on HOC partitioning.

$$S_{HOC} = (0.004C_{\text{HOC}}) \qquad \text{for } C_s < 0.78 \text{ m}M \tag{7}$$

$$S_{\text{HOC}} = \left(\frac{1}{[159000C_s - 125]}\, C_{\text{HOC}}\right) \tag{8}$$

$$\text{for } C_s \geq 0.78 \text{ m}M$$

Nonequilibrium Sorption

Two-domain approach. For nonequilibrium sorption processes, (3), (4), and (5) must be modified to account for the kinetics of sorption. A two-domain approach has been used successfully to describe heterogeneities and/or nonequilibrium sorption of HOCs in groundwater transport models [*Goltz and Roberts*, 1986; *Brusseau et al.*, 1991]. The two-domain or bicontinuum approach depicts sorption as occurring in two compartments: one compartment governed by an instantaneous (equilibrium) sorption process, with a sorbed concentration (S_1), and the second governed by a first-order, reversible, nonequilibrium sorption process, with a sorbed concentration (S_2). The overall process can be represented by

$$C \overset{g(C)}{\leftrightarrow} S_1 \underset{k_2}{\overset{k_1}{\rightleftharpoons}} S_2 \tag{9}$$

where k_1 and k_2 are first-order forward and reverse rate constants.

Sorption in the two domains is governed by the following equations [*Brusseau et al.*, 1991]:

$$S_1 = Fg(C) \tag{10}$$

$$\frac{dS_2}{dt} = k_2[(1 - F)g(C) - S_2] \tag{11}$$

The total sorbed mass at equilibrium is the sum of the mass present in each domain is given as

$$S = S_1 + S_2 = Fg(C) + (1 - F)g(C) = g(C) \tag{12}$$

where F represents the fraction of sorbed mass that attains instantaneous equilibrium with the aqueous-phase concentration. Here (11) can be solved by using the Euler–Cauchy (predictor) method. The sorption module then comprises the following two nonlinear simultaneous equations which are solved simultaneously for $S_{2,i}^{*t+1}$ and C_i^{*t+1} using the Bisection method [*Press et al.*, 1992].

$$S_{2,i}^{*t+1} = S_{2,i}^{t} + \Delta t k_2[(1 - F)g(C_i^t) - S_{2,i}^t] \tag{13}$$

$$M_i^{t+1} = \theta C_i^{*t+1} + \rho F g(C_i^{*t+1}) + \rho S_{2,i}^{*t+1} \tag{14}$$

Two-stage approach. Sorption of nonionic surfactants onto solid media is typically nonlinear [*Partyka et al.*, 1984; *Somasundaran et al.*, 1991]. Equilibrium sorption of Triton X-100 ($C_8PE_{9.5}$), a nonionic surfactant, onto Lincoln fine sand has been characterized by a Langmuir isotherm [*Adeel and Luthy*, 1995].

$$S_s = g(C_s) = \frac{S_{\max} K_l C_s}{[1 + K_l C_s]} \tag{15}$$

where S_s is the mass of surfactant sorbed per unit weight of the soil (MM^{-1}), $S_{\max}$ is the maximum sorbed surfactant concentration (MM^{-1}), C_s is the aqueous-phase surfactant concentration (ML^{-3}), and K_l is the Langmuir constant (L^3M^{-1}).

It was proposed by *Adeel and Luthy* [1995] that the sorption kinetics of Triton X-100 onto Lincoln fine sand are governed by two sequential sorption regimes. The sorption kinetics in each regime are dependent on the molecular conformation of the sorbed surfactant and the nature of molecular interaction. Mathematically,

$$C_s \underset{k_{b1}}{\overset{k_{f1}}{\rightleftharpoons}} S_a \tag{16}$$

$$C_s \underset{k_{b2}}{\overset{k_{f2}}{\rightleftharpoons}} S_b \tag{17}$$

where k_f and k_b are first-order forward and reverse rate constants, and subscripts 1 and 2 represent the corresponding sorption regime. It is assumed in the first stage the sorbed surfactant concentration (S_a) is sparse and sorption is governed by surfactant–surface interactions ($S_a \leq 2.4$ μmol/g), whereas the sorption in the second stage (S_b) is close to saturation and is assumed to be governed by surfactant–surfactant interactions. These assumptions result in two simplified equations, (18) and (19), that comprise the sorption module [*Adeel and Luthy*, 1995].

$$\frac{dC_s}{dt} = -k_{f1}C_s \qquad \text{for } 0.0 \leq S_s < 2.4 \text{ } \mu\text{mol/g} \tag{18}$$

$$\frac{dC_s}{dt} = \frac{-k_{b2}\rho}{\theta}\{[g(C_s) - S_a] - S_b\} \tag{19}$$

$$\text{for } 2.4 \text{ } \mu\text{mol/g} \leq S_s < 6.5 \text{ } \mu\text{mol/g}$$

whereas the term $g(C_s) - S_a$ represents the maximum sorption in the second regime corresponding to equilibrium, and thus the term in braces on the right side of (19) may be visualized as a driving force term for the second sorption re-

gime. These differential equations are solved iteratively using the Euler–Cauchy (predictor) method considering mass conservation.

$$C_s^{t+1} = C_s^t - k_{f1}\Delta t C_s^t \tag{20}$$

$$M_i^{t+1} = \theta C_s^{*t+1} + \rho S_a^{*t+1} + \rho S_b^{*t+1} \tag{21}$$

$$S_a^{*t+1} = \frac{1}{\rho}[M^{t+1} - \theta C_s^{*t+1}] \tag{22}$$

$$S_b^{*t+1} = \frac{1}{\rho}[M^{t+1} - \theta C_s^{*t+1} - \rho S_a^t] \tag{23}$$

Parameter Estimation

The parameters describing a nonlinear, nonequilibrium sorption module may not always be readily available from laboratory experiments [*Brusseau et al.*, 1991]. This problem can be overcome by using conventional parameter estimation methods to fit results from the STSS model to experimental data. An iterative search method developed by *Marquardt* [1963], known as the Levenberg–Marquardt algorithm, is used here for estimation of parameter values in the nonequilibrium models. This method varies smoothly between extremes of the inverse Hessian method and the steepest descent method, due to a nondimensional scaling factor being varied after each iteration [*Press et al.*, 1992]. It provides good convergence for cases where initial estimates for the parameters provide model output values close to the data being fitted.

The parameters of the model are adjusted to achieve a minimum in a chosen measure of error, referred to as a merit function (P) between the observed values and the model estimates. The merit function used here is a relative least squares (RLS) function, described as [*Ramila*, 1990]

$$P = \sum_{i=1}^{N} \left(\frac{C - \hat{C}}{C}\right)_i^2 \tag{24}$$

where N is the number of observations, C is the observed aqueous concentration value, and $\hat{C}$ is the predicted value of the concentration. The appendix provides details of the mathematical derivation of the expressions used in the Levenberg–Marquardt algorithm for the two-domain model.

Experimental Methods

Materials

Triton X-100 (C_8H_{17}-C_6H_4-$O(CH_2CH_2O)_{9.5}H$) was selected as a representative nonionic surfactant because of its ability to enhance solubilization of organic compounds [*Edwards et al.*, 1994], its having been studied by other researchers [*Robson and Dennis*, 1977; *Partyka et al.*, 1984; *Somasundaran et al.*, 1991], and its availability in radiolabeled form. The ^{3}H-Triton X-100 was obtained from New England Nuclear (NEN), E. I. DuPont de Nemours and Company, Inc. and in nonlabeled form from Aldrich Chemical Company; the radiolabeled and nonlabeled surfactant were mixed in known proportions. The critical micelle concentration (CMC) of Triton X-100 with 0.01 M $CaCl_2$ was determined to be 1.8×10^{-4} mol/L from surface tension measurements [*Edwards et al.*, 1994]. The ^3H_2O was obtained from DuPont NEN.

Phenanthrene was selected as a representative HOC because of its low volatility and relatively high hydrophobicity. Radiocarbon-labeled phenanthrene was obtained from Sigma Chemical Company and in nonlabeled form with a 98% purity from Aldrich Chemical Company. All aqueous solutions contained 0.01 M $CaCl_2$ in order to prevent migration of fines by providing uniform ionic strength conditions.

Clean, Lincoln fine sand passing U.S. standard sieve 10 (2 mm) was used as the sediment material. The sand was air-dried before shipment from U.S. Environmental Protection Agency (EPA) Robert S. Kerr Environmental Research Laboratory, Ada, Oklahoma. The Walkley–Black method [*Nelson and Sommers*, 1986] was used to determine the fractional organic carbon in Lincoln fine sand; this value was found to be 0.05%, consistent with a value of 0.034% reported by *Wilson et al.* [1981]. The surface area for Lincoln fine sand was calculated from nitrogen adsorption data in accordance with the Brunauer, Emmett, and Teller (BET) adsorption theory [*Gregg and Sing*, 1967]. The surface area was found to be 3.0 m^2/g.

Liquid Scintillation Counting

The aqueous-phase concentrations of ^3H_2O, Triton X-100, and phenanthrene were determined by measuring ^3H or ^{14}C disintegrations per minute. The liquid samples ranged in volume from 0.1 mL to 1.0 mL and were mixed with 10.0 mL Packard Optifluor scintillation cocktail in 20.0 mL polyethylene vials. These samples were then analyzed in a Beckman LS 5000 TD liquid scintillation counter for radioactivity.

Column Transport Experiments

The column transport experiments were performed in a stainless steel column with a transport length of 7.53 cm and an inner diameter of 2.20 cm, packed with 49.75 ± 1.00 g Lincoln fine sand. The sand was placed in the column in 18–20 layers, and the bulk density of the sand was determined to be 1.74 ± 0.04 g/cm^3. The column was flushed with water until fully saturated, and the pore volume of the packed column was determined by the weight difference of the water-saturated column versus the dry column; the porosity was determined to be between 0.34 and 0.37. Stainless steel frits with 0.5 μm pore size were used at both ends of the column to prevent migration of fine particles. The column apparatus and the related equipment were designed in such a way that the surfaces contacted by the aqueous solutions were either stainless steel, Teflon, or glass. The aqueous solutions for column tests were sparged with helium prior to pumping, in order to remove any entrapped air bubbles. A Scientific Systems, Inc. SSI Model 350 liquid chromatography pump was used to pump aqueous solutions from the reservoir. The effluent from the column was collected by an Eldex fraction collector in 10-mL glass tubes. The volume of the liquid collected in the glass tubes depended on the flow rate and the frequency of observations.

The column was cleaned and repacked for each separate run. A newly filled column was conditioned in all instances by pumping 500 mL or more of 0.01 M $CaCl_2$ solution in order to obtain steady state flow conditions, and to remove any spurious suspended colloids. After the conditioning, a ^3H_2O solution with 0.01 M $CaCl_2$ was pumped through the column and monitored at the outlet. The breakthrough curve from the ^3H-water flushing was used to estimate dispersivity of the sediment column by fitting the advection–dispersion transport equation to the data. The column was then purged with 0.01 M $CaCl_2$ solution until the ^3H count was reduced to background level. The radiolabeled Triton X-100 or phenanthrene solutions

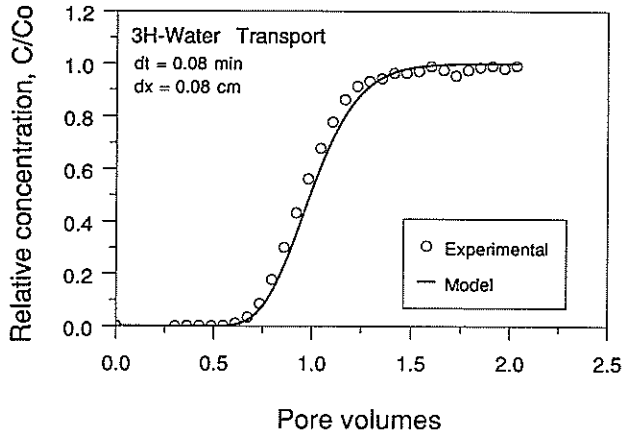

Figure 4. Prediction of ^3H_2O transport by the STSS numerical approach. Simulated for flow of a conservative tracer through the column described in Figure 2.

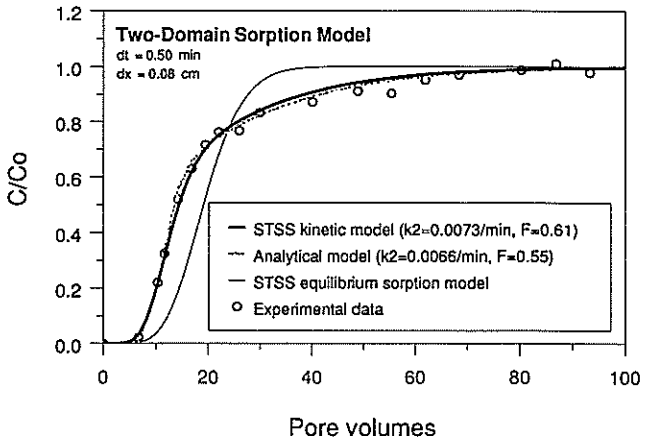

Figure 5. The breakthrough curve for transport of phenanthrene in Lincoln fine sand. Phenanthrene was flushed through a 2.20-cm ID, 7.53-cm-long column with average pore water velocity of 0.81 cm/min, dispersivity of 0.15 cm, and porosity of 0.37.

were then pumped. In between different column runs, the stainless steel reservoir and the tubing leading to the column were cleansed with a methanol solution followed by distilled water.

Model Simulations

No Sorption

Here ^{3}H-water containing 0.01 M $CaCl_2$ was used as a nonreactive, conservative tracer. The data from a column experiment are shown in Figure 4 along with the predicted curve from the STSS technique; such a behavior is expected of a conservative tracer [*Parker and van Genuchten*, 1984]. The volume of the tracer solution required for a complete breakthrough was computed to be equal to one pore volume by numerically integrating the area to the left of the curve. Before using the STSS technique, an estimate of the longitudinal dispersivity (α) was obtained by fitting an analytical solution of the advection–dispersion equation to the experimental data [*Parker and van Genuchten*, 1984]. The α value was determined to be 0.15 cm, which agrees well with the reported longitudinal dispersivity value of 0.13 cm for a laboratory experiment comprising aqueous solution transport through a Lincoln fine sand column [*Liu et al.*, 1991].

Nonequilibrium, Linear Sorption

HOCs may undergo nonequilibrium sorption during transport [*Brusseau et al.*, 1991]. In this paper, data for nonequilibrium sorption and transport of phenanthrene in a column containing Lincoln fine sand are modeled with a two-domain model. The column was flushed with a phenanthrene solution having a 4-m*M* aqueous phase concentration, slightly below its solubility limit. The breakthrough curve presented in Figure 5 shows a behavior typical of nonequilibrium sorption: a retarded breakthrough followed by prolonged tailing, and with more than 80 pore volumes required to achieve a complete breakthrough. A linear equilibrium isotherm (K_d = 0.004 L/g) for sorption of phenanthrene onto Lincoln fine sand was used in modeling nonequilibrium transport of phenanthrene [*Edwards*, 1993].

A two-domain sorption module using (13) and (14) was employed in modeling the data. Figure 5 shows a reasonable fit by the STSS approach, where k_2 = 0.0073/min and F = 0.61. The analytical two-domain model provided by *Parker and van Genuchten* [1984] was also used to fit the data for k_2 and F. A very close agreement among the STSS model, the analytical model, and the experimental data was found. As a comparison, the output from an equilibrium transport model using (4) and (5) is also shown in Figure 5. It can be observed that the equilibrium assumption (Type 1 model) is inappropriate in this case.

Nonequilibrium, Two-Stage Sorption

The two-stage nonequilibrium sorption module using (20)–(23) is used to predict flushing of a Lincoln fine sand column by a Triton X-100 solution at 8.9 m*M*, 50 times its CMC, using k_{f1} and k_{b2} as fitting parameters. Initial estimates of k_{f1} and k_{b2} were obtained by using the Levenberg-Marquardt algorithm. Here (15) was used as the equilibrium sorption isotherm in the corresponding mathematical model (K_l = 967 L/mol, S_{max} = 6.5 × 10^{-6} mol/g). The fitted curve and the experimental data are shown in Figure 6 [*Adeel and Luthy*, 1995] for

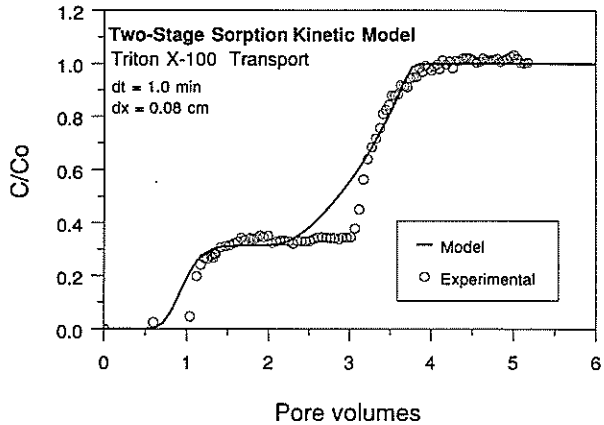

Figure 6. The breakthrough data for transport of Triton X-100 in Lincoln fine sand; the STSS technique was used to predict surfactant transport according to a two-step kinetic model. Triton X-100 was flushed through a 2.20-cm ID, 7.53-cm-long column with average pore water velocity of 0.02 cm/min, dispersivity of 0.15 cm, and porosity of 0.34.

$k_{f1} = 3.7 \times 10^{-3}$/min and $k_{b2} = 9.0 \times 10^{-7}$/min. The dispersivity of the column was estimated by conservative tracer transport, as described previously. The surfactant sorption model as applied by the STSS technique provided a reasonable fit for the breakthrough data and captured most of the salient features of the two-step surfactant breakthrough curve.

Equilibrium, Interactive Sorption

Equilibrium modules for sorption of phenanthrene and Triton X-100 are assumed for demonstration purposes. It is understood that sorption for either phenanthrene or Triton X-100 may typically be a nonequilibrium process at the pore water velocities usually encountered under natural conditions. This simulation will illustrate the case that may be relevant to extremely slow pore water flow velocities where local equilibrium assumption is valid.

Figure 7 shows model prediction for coupled transport of phenanthrene and Triton X-100 under equilibrium conditions. Also plotted on the same figure are experimental data for phenanthrene transport in a sand column that was initially saturated with phenanthrene at 4 mM and then flushed by the surfactant at 26 mM, 150 times the CMC. The predicted curve describes the observed peak in phenanthrene concentration quite well. The model prediction, however, fails to simulate the long tailing in phenanthrene concentration. The complete removal of phenanthrene in about four pour volumes, as was simulated, can be attributed to the equilibrium assumption in the model; this indicates that an equilibrium approach for modeling surfactant-enhanced flushing of HOCs may not be appropriate.

Nonequilibrium, Interactive Sorption

Nonequilibrium surfactant-enhanced flushing of phenanthrene from Lincoln fine sand with Triton X-100 is simulated using the numerical STSS approach. The sorption module for phenanthrene is based on (7), (8), (13), and (14). A two-stage, nonlinear sorption module comprising (20)–(23) governs the surfactant transport [*Adeel and Luthy*, 1995]. These two sorption modules are then evaluated in series with the transport module for simultaneous nonequilibrium transport of both phenanthrene and Triton X-100.

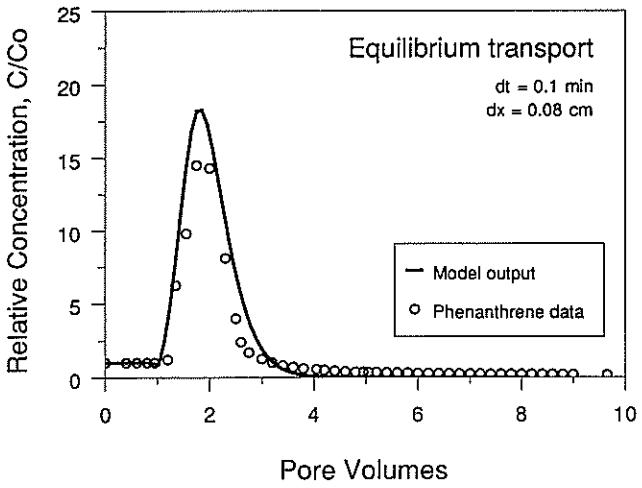

Figure 7. Experimental data and simulated flushing of phenanthrene by a nonionic surfactant, Triton X-100, assuming equilibrium sorption. The surfactant solution was flushed through a 2.20-cm ID, 7.53-cm-long column with average pore water velocity of 0.80 cm/min, dispersivity of 0.15 cm, and porosity of 0.37.

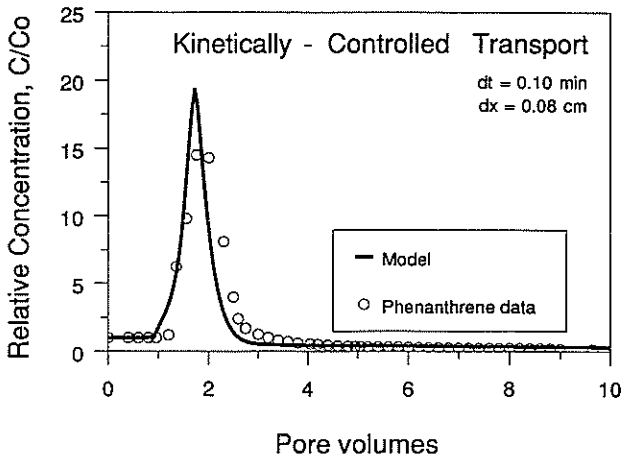

Figure 8. Experimental data and predicted flushing of phenanthrene by a nonionic surfactant, Triton X-100. The STSS technique was used to couple two-domain phenanthrene sorption kinetics with two-step Triton X-100 sorption kinetics. The surfactant solution was flushed through a 2.20-cm ID, 7.53-cm-long column with average pore water velocity of 0.80 cm/min, dispersivity of 0.15 cm, and porosity of 0.37.

The simulated relative bulk solution concentration of phenanthrene is plotted in Figure 8, along with experimental data, as a function of pore volumes of surfactant solution flushed through the column. The predicted curve follows the experimental data quite closely such that a large mass (~71%) of phenanthrene is initially flushed through the column, followed by prolonged tailing at low concentrations. The difference in the peak shapes between the experimental observations and the simulations indicates that although surfactant and phenanthrene transport are kinetically controlled, the coupled phenomena are not completely captured by the model in its present form.

Multicomponent Nonequilibrium, Linear Sorption

Multiple organic compounds are often present in contaminated aquifers [*Mackay and Cherry*, 1989; *Feenstra*, 1992]. For simulation of multicomponent transport, it is assumed that solubilization and sorption of each compound is independent of the presence of others (Type 4 transport). Such an assumption is reasonable for hydrophobic compounds like polychlorinated biphenyls (PCBs), since solute–water interactions dominate the behavior of the dissolved compounds and the solute–solute interactions are not significant owing to high dilution [*Mackay et al.*, 1991].

A simulation of one-dimensional transport of a sorbed-phase PCB mixture (similar to Aroclor 1016) is performed; the transport of different PCB congeners is predicted from a contaminated source region 2 m wide, with Aroclor 1016 initially present at the source as a sorbed mass of 1000 mg/kg. Salient physical and chemical properties of Aroclor 1016 are shown in Table 1. The aroclor is treated as a mixture of five homologous congener groups. Biphenyl and hexachlorobiphenyl are excluded from the simulation owing to their low mass fraction in the aroclor mixture.

The sorption of PCB congener groups is considered to be a nonequilibrium process represented by a two-domain sorption

Table 1. Physico-Chemical Properties of Aroclor 1016

Congener Group[a]	Fraction, % by mass	Log K_{ow}	Molecular Weight
Biphenyl (1)	<0.1	3.9	154.2
Monochlorobiphenyl (3)	1	4.5	188.7
Dichlorobiphenyl (12)	20	5.1	223.1
Trichlorobiphenyl (24)	57	5.8	257.5
Tetrachlorobiphenyl (42)	21	6.0	292.0
Pentachlorobiphenyl (46)	1	6.4	326.0
Hexachlorobiphenyl (42)	<0.1	7.0	360.9

Properties from [*Shiu and Mackay*, 1986]
[a]Values in parentheses represent number of isomers in the group.

model. The equilibrium sorption isotherm for each congener group is correlated to an averaged octanol-water partition coefficient (K_{ow}) [*Oliver*, 1985].

$$\log K_P = 0.41 \log K_{ow} + 1.5 \quad (25)$$

where K_P is the partition coefficient (mL/g) for a PCB congener group. The two parameters for two-domain sorption model, k_{2P} and F_P, are determined by using quantitative structure activity relationships developed by *Brusseau et al.* [1991].

$$\log k_{2P} = 24(1 - 0.825 \log (1000\ K_P)) \quad (26)$$

$$F_P = -0.2265 + 0.1215 \log K_{ow} \quad (27)$$

The concentration profiles away from the contaminant source are presented in Figures 9 and 10 for each of the congener group, at 5,000 and 10,000 days, respectively. The profiles shown in these figures suggest that the concentration of each PCB congener group is dependent on its mass fraction in the Aroclor mixture and the degree of chlorination. The simulated transport distances for all five congener groups are, however, similar.

Discussion

Conventional modeling techniques for solute transport in porous media cannot accommodate spatial and temporal variations in partitioning phenomena arising from multiple solute interactions. Such variations may arise owing to kinetic interactions among different solutes or to the presence of surfactants or other solubilizing agents. The segregated transport-sorption/solubilization (STSS) technique provides the capability for handling such multicomponent transport problems. Coupled to the Levenberg–Marquardt algorithm for parameter estimation, the STSS approach becomes a deterministic tool for describing experimental data.

Precise values of the parameters k_2 and F used in the two-domain models, or the parameters k_{f1} and k_{b2} used in the two-stage surfactant sorption model, can be determined with the Levenberg–Marquardt algorithm. This algorithm is often associated with numerical modeling problems and provides good convergence when initial parameter estimates allow for close approximation of the experimental data. However, its performance is limited when model predictions are relatively divergent from the experimental data and the computed merit function is accordingly large. In this study, initial estimates of parameters were made by a trial and error execution of STSS, where one parameter was incremented while keeping the other constant until no further improvement in the output was observed. These initial estimates were then polished to final values by using the Levenberg–Marquardt algorithm.

The predictive capability of the STSS technique is displayed for simulated surfactant flushing of phenanthrene from Lincoln fine sand. As a first approximation, it is assumed that the sorption phenomena of phenanthrene and Triton X-100 are independent of each other. A more rigorous approach would be to consider the variation in the kinetic behavior of surfactant and/or HOC sorption as a function of surface coverage by these compounds. The micellar Triton X-100 solution is capable of significantly enhancing the apparent solubility (in this case up to 15 times the aqueous solubility) of phenanthrene by its uptake in the micellar pseudophase. However, experimental evidence suggests that continued flushing of HOC-contaminated aquifer media with surfactant solution would result in prolonged desorption and a slow mass removal after the initial high-concentration flush.

A modeling approach that assumes equilibrium sorption for both phenanthrene and the surfactant predicts the high-concentration peak but fails to predict the prolonged desorption. This prediction of complete phenanthrene removal in a few pore volumes is based on the assumption of local equilibrium between different phases; such a prediction appears to be unrealistic when compared against experimental data. However, a modeling approach that assumes independent sorption kinetics for phenanthrene and the surfactant predicts both the initial high concentration phenanthrene flush and the subsequent prolonged desorption. A comparison of the two modeling approaches emphasizes the importance of characterizing coupled kinetic phenomena.

The simulated transport of PCB congener groups (Figures 9 and 10) suggests some interesting results. In general, PCB compounds have low aqueous solubility and a high degree of hydrophobicity, which means that their transport in saturated aquifers should be slow and that the interactions among different congeners should be minimal. The extent of retardation of a congener group is related to its mass fraction in the Aroclor mixture and its degree of chlorination, which in turn controls the equilibrium partitioning as well as the kinetics of the sorption phenomena. The prediction using the STSS technique shows that there is very little movement of PCB congener groups during the time scales considered (15–30 years). Slow desorption from the contaminated zone and strong sorp-

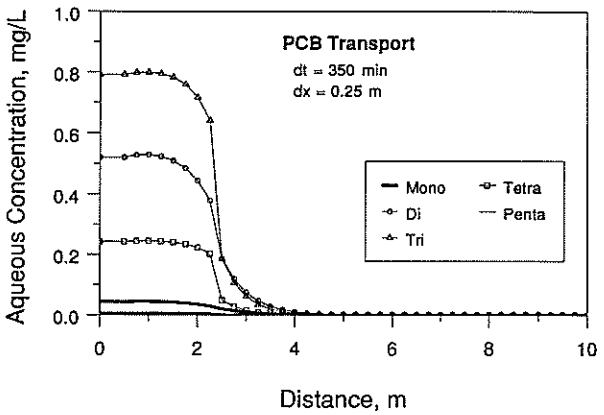

Figure 9. Simulated transport of PCB congeners for Aroclor 1016 after 5000 days from a contaminated region 2 m long, with an average pore water velocity of 0.1 m/d, porosity of 0.3, f_{oc} of 0.001, and dispersivity of 10 m.

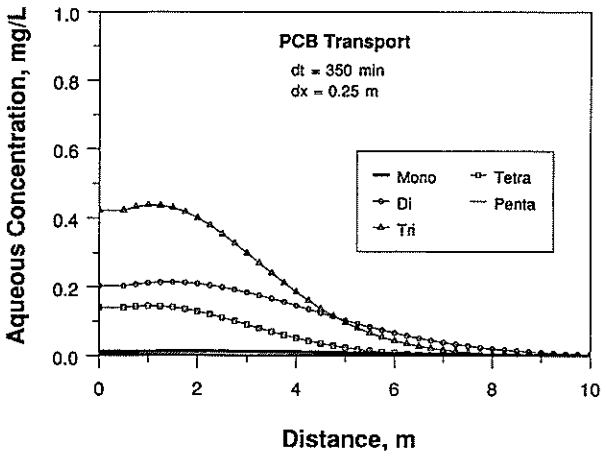

Figure 10. Simulated transport of PCB congeners for Aroclor 1016 after 10000 days from a contaminated region 2 m long, with an average pore water velocity of 0.1 m/d, porosity of 0.3, f_{oc} of 0.001, and dispersivity of 10 m.

tion onto the clean sand appears to severely restrict the movement of PCB. Such a prediction, coupled with supporting experimental evidence, can provide very useful insight into plume containment strategies for PCB-contaminated aquifers. In this simulation study, no pure phase PCB or facilitated transport was considered, which may be significant in field situations.

The scope of STSS modeling technique can be expanded to assess other transport phenomena. The sorption of HOCs onto colloidal particles and macromolecules may serve as a mechanism for enhanced mobility of organic contaminants in groundwater [*Magee et al.*, 1991]. These colloidal particles may be mostly organic in nature, and the HOCs may tend to partition onto these colloids just as they would onto aquifer sediments. One approach for addressing this situation considers the enhancement in transport of HOC by modifying the advective transport in (2) as [*Dzombak et al.*, 1994].

$$\frac{\rho}{\theta}\frac{\partial S}{\partial t} + \frac{\partial C}{\partial t} = D\frac{\partial^2 C}{\partial x^2} - v(1 + K_{oc}C_{oc})\frac{\partial C}{\partial x} \qquad (28)$$

where K_{oc} is the coefficient for HOC partitioning onto the colloids, and C_{oc} is the concentration of the colloids in water. The formulation in (28) assumes that the colloids are completely "mobile" (i.e., are not sorbed or physically retained by the solid media), and that the sorption of HOC onto colloids is completely reversible. In the STSS model the enhanced advective transport due to colloids can be accounted for by increasing the average pore water velocity v by a factor of $(1 + K_{oc}C_{oc})$.

The dissolution from a nonaqueous phase liquid (NAPL) is an important process at many contamination sites, where contaminants may exist in a residual saturation even after preliminary pump-and-treat cleanup. The kinetics of dissolution from a NAPL phase to the aqueous phase can be modeled as a typical mass transfer problem as shown below [*Dzombak et al.*, 1994].

$$\frac{dC}{dt} = \frac{k_n a}{S_w}(C_{eq} - C) \qquad (29)$$

where C_{eq} is the equilibrium concentration of a component of the organic liquid-phase in accordance with the Raoult's law, k_n is the mass transfer coefficient for a component, a is the surface area of the NAPL in contact with the aqueous phase, and S_w is the water saturation in pore voids. Dissolution from pure phase liquids or mixtures can be incorporated into a sorption module or can be treated as a separate module as given by (29).

In practice, groundwater transport modeling also has to account for longitudinal and transverse components of advective velocity and hydrodynamic dispersivity. In principal, there is no mathematical limitation to extension of the transport module in the STSS technique to accommodate such two- or three-dimensional flow problems.

Appendix: Determination of Derivatives for Levenberg–Marquardt Algorithm (Two-Domain Sorption Model).

The values of the first partial derivatives can be obtained by differentiating (24),

$$\beta_{k_2} = \frac{\partial P}{\partial k_2} = \sum_{i=1}^{N}\frac{-2}{C_i^2}\left[(C - \hat{C})_i\frac{\partial \hat{C}_{k_2}}{\partial k_2}\right] \qquad (A1)$$

$$\beta_F = \frac{\partial P}{\partial F} = \sum_{i=1}^{N}\frac{-2}{C_i^2}\left[(C - \hat{C})_i\frac{\partial \hat{C}_F}{\partial F}\right] \qquad (A2)$$

Taking an additional partial derivative of (A1) gives

$$\alpha_{Fk_2} = \frac{\partial^2 P}{\partial F\partial k_2} = \sum_{i=1}^{N}\frac{-2}{C_i^2}\left[\frac{-\partial \hat{C}_F}{\partial F}\cdot\frac{\partial \hat{C}_{k_2}}{\partial k_2} + (C - \hat{C})_i\frac{\partial^2 \hat{C}}{\partial F\partial k_2}\right] \qquad (A3)$$

The second-order partial derivatives in (A3) can be simplified by using the Gauss–Newton method [*Seinfeld and Lapidus*, 1974]. According to this method, the second term in (A3) is a product of the error term $(C - \hat{C})$ and a second-order partial derivative, and can be ignored as being small, particularly so when the estimates are close to the observed data. Hence, (A3) can be approximated as

$$\alpha_{Fk_2} = \frac{\partial^2 P}{\partial F\partial k_2} = \sum_{i=1}^{N}\frac{2}{C_i^2}\left[\frac{\partial \hat{C}_F}{\partial F}\cdot\frac{\partial \hat{C}_{k_2}}{\partial k_2}\right] = \frac{\partial^2 P}{\partial k_2\partial F} = \alpha_{k_2F} \qquad (A4)$$

Similarly,

$$\alpha_{k_2k_2} = \frac{\partial^2 P}{\partial k_2^2} = \sum_{i=1}^{N}\frac{2}{C_i^2}\left[\frac{\partial \hat{C}_{k_2}}{\partial k_2}\right]^2 \qquad (A5)$$

and

$$\alpha_{FF} = \frac{\partial^2 P}{\partial F^2} = \sum_{i=1}^{N}\frac{2}{C_i^2}\left[\frac{\partial \hat{C}_F}{\partial F}\right]_i^2 \qquad (A6)$$

The partial derivatives of the concentration $\hat{C}$ with respect to the fitting parameter cannot be obtained analytically for a nonlinear, nonequilibrium process. In order to obtain these partial derivatives numerically, one parameter is held constant while the other is changed by a small increment (Δk_2 and ΔF).

$$\frac{\partial \hat{C}_{k_2}}{\partial k_2} = \sum_{i=1}^{N} \left(\frac{\hat{C} - \hat{C}_{k_2}}{\Delta k_2} \right)_i \quad \text{(A7)}$$

$$\frac{\partial \hat{C}_F}{\partial F} = \sum_{i=1}^{N} \left(\frac{\hat{C} - \hat{C}_F}{\Delta F} \right)_i \quad \text{(A8)}$$

where $\hat{C}_{k_2}$ and $\hat{C}_F$ denote the model predictions obtained after incrementing k_2 and F.

Notation

α_{lm} second partial derivative of the merit function with respect to fitting parameters.
β_l first partial derivative of the merit function with respect to a fitting parameter.
θ porosity of the soil (dm^3/dm^3).
ρ bulk density of soil (g/dm^3).
a surface area of NAPL in contact with the aqueous phase (cm^2).
C flux-averaged aqueous-phase solute concentration (mol/L).
C_{eq} equilibrium aqueous concentration of a component from an organic liquid phase (mol/L).
C_{HOC} flux-averaged aqueous-phase concentration of phenanthrene (mol/L).
C_{oc} concentration of organic colloidal particles in water (g/L).
C_s flux-averaged aqueous-phase concentration of Triton X-100 (mol/L).
$\hat{C}$ predicted value of effluent concentration (mol/L).
D hydrodynamic dispersion coefficient (cm^2/min).
F fraction of mass sorbed instantenously (dimensionless).
$k_{1,2}$ first-order forward or reverse rate constant (1/min).
$k_{f1,2}$ first-order forward rate constant in surfactant sorption regime 1 or 2 (1/min).
$k_{b1,2}$ first-order reverse rate constant in surfactant sorption regime 1 or 2 (1/min).
k_n mass transfer coefficient for a component ($1/cm^2 \cdot$ min).
K_l Langmuir constant for surfactant sorption isotherm (L/g).
K_{oc} partition coefficient of HOC between colloids and the aqueous phase (L/g).
K_d partition coefficient for phenanthrene between solid and aqueous phase (L/g).
K_{ow} octanol-water partition coefficient (dimensionless).
K_p partition coefficient for PCB congener between solid and aqueous phase (L/kg).
M total solute mass per volume of a cell (mol/L).
N number of observations to be fitted by parameter estimation.
P merit function for parameter estimation, RLS (dimensionless).
S concentration of solute sorbed onto soil (mol/g).
S_1 sorbed mass per unit weight of soil in equilibrium domain (mol/g).
S_2 sorbed mass per unit weight of soil in nonequilibrium domain (mol/g).
$S_{a,b}$ sorbed mass per unit weight of soil in surfactant sorption regime 1 or 2 (mol/g).
S_{HOC} mass of sorbed HOC (phenanthrene) per unit weight of soil (mol/g).
S_s mass of sorbed Triton X-100 per unit weight of soil (mol/g).
$S_{\max}$ maximum mass of sorbed Triton X-100 per unit weight of soil (mol/g).
S_w water saturation in pore voids containing NAPL (L/L).
t time (min).
Δt time step for finite differencing (min).
v average pore water velocity (cm/min).
x distance from the inlet boundary (cm).
Δx assumed size of a cell in the flow domain (cm).

Acknowledgments. This research was supported by the U.S. Environmental Protection Agency, Office of Exploratory Research, Washington, D. C., through grant R819266-01-0. Additional funding was provided by the Alcoa Environmental Technology Center, Pittsburgh, PA. John Smith was the Project Officer for Alcoa.

References

Abdul, A. S., and T. L. Gibson, Laboratory studies of surfactant-enhanced washing of polychlorinated biphenyl from sandy material, *Environ. Sci. Technol.*, *25*(4), 665–671, 1991.

Abdul, A. S., T. L. Gibson, and D. N. Rai, Selection of surfactants for the removal of petroleum products from shallow sandy aquifers, *Ground Water*, *28*, 920–926, 1990.

Adeel, Z., and R. G. Luthy, Sorption and transport kinetics of a nonionic surfactant through an aquifer sediment, *Environ. Sci. Technol.*, *29*(4), 1032–1042, 1995.

Brusseau, M. L., Rate-limited mass transfer and transport of organic solutes in porous media that contain immobile immiscible organic liquid, *Water Resour. Res.*, *28*(1), 33–45, 1992.

Brusseau, M. L., R. E. Jessup, and S. C. Rao, Nonequilibrium sorption of organic chemicals: Elucidation of rate-limiting processes, *Environ. Sci. Technol.*, *25*(1), 134–142, 1991.

Cederberg, G. A., R. L. Street, and J. O. Leckie, A groundwater mass transport and equilibrium chemistry model for multicomponent systems, *Water Resour. Res.*, *28*(1), 33–45, 1992.

Dzombak, D. A., R. G. Luthy, Z. Adeel, and S. B. Roy, Modeling transport of PCB congeners in the subsurface, *Final Rep. to Aluminum Company of America*, Alcoa Center, Environmental Technology Center, Alcoa Center, Pa., 1994.

Edwards, D. A., Nonionic surfactant effects on the distribution of hydrophobic organic compounds in aqueous, soil/aqueous and sediment/aqueous systems, Ph.D. thesis, Carnegie Mellon Univ., Pittsburgh, Pa., 1993.

Enfield, C. G., R. F. Carsel, and S. Z. Cohen, Approximating pollutant transport to ground water, *Ground Water*, *20*, 711–722, 1982.

Feenstra, S., Evaluation of multi-component DNAPL source by monitoring of dissolved-phase concentrations, *Proceedings of the International Conference of Subsurface Contamination of Immiscible Fluids, Calgary, Canada, April 18–20, 1990. Subsurface Contamination by Immiscible fluids*, edited by K. U. Weyer, A. A. Balkema, Brookfield, Vt., 1992.

Goltz, M. N., and P. V. Roberts, Interpreting organic solute data from a field experiment using physical nonequilibrium models, *J. Contam. Hydrol.*, *1*(1/2), 77–93, 1986.

Gregg, S. J., and K. S. W. Sing, *Adsorption Surfaces Area and Porosity*, Academic, San Diego, Calif., 1967.

Grove, D. B., and K. G. Stollenwerk, Computer model of one-dimensional equilibrium controlled sorption processes, *U.S. Geol. Surv. Water Resour. Invest. Rep. 84-4059*, U.S. Geol. Surv., Denver, Colo., 1984.

Grove, D. B., and W. W. Wood, Prediction and field verification of subsurface-water quality changes during artificial recharge, Lubbock, TX, *Ground Water*, *17*(3), 250–257, 1979.

Holsen, T. M., E. R. Taylor, Y-C. Seo, and P. R. Anderson, Removal of sparingly soluble organic chemicals from aqueous solutions with surfactant-coated ferrihydrite, *Environ. Sci. Technol.*, *25*(9), 1585–1589, 1991.

Lee, J-F., J. R. Crum, and S. A. Boyd, Enhanced retention of organic contaminants by soil exchanged with organic cations, *Environ. Sci. Technol.*, *23*(11), 1365–1372, 1989.

Liu, K-H., C. G. Enfield, and S. C. Mravik, Evaluation of sorption models in the simulation of naphthalene transport through saturated soils, *Ground Water*, *29*, 685–692, 1991.

Mackay, D. M., and J. A. Cherry, Groundwater contamination: Pump-and-treat remediation, *Environ. Sci. Technol.*, *23*(6), 630–636, 1989.

Mackay, D. M., W. Y. Shiu, A. Maijanen, and S. Feenstra, Dissolution of non-aqueous phase liquids in groundwater, *J. Contam. Hydrol.*, *8*, 23–42, 1991.

Magee, B. R., L. W. Lion, and A. T. Lemley, Transport of dissolved organic macromolecules and their effect on the transport of phenanthrene in porous media, *Environ. Sci. Technol.*, *25*(2), 323–331, 1991.

Marquardt, D. W., An algorithm for least-squares estimation of nonlinear parameters, *J. Soc. Ind. Appl. Math.*, *11*(2), 431–441, 1963.

McRae, G. J., W. R. Goodin, and J. H. Seinfeld, Numerical solution of the atmospheric diffusion equation for chemically reacting flows, *J. Comput. Phys.*, *45*, 1–42, 1982.

Molz, F. J., M. A. Widdowson, and L. D. Benefield, Simulation of microbial growth dynamics coupled to nutrient and oxygen transport in porous media, *Water Resour. Res.*, *22*(8), 1207–1216, 1986.

Nelson, D. W., and L. E. Sommers, Total carbon, organic carbon, and organic matter, in *Methods of Soil Analysis, 2, Chemical and Microbiological Properties*, edited by A. L. Page, pp. 539–579, Am. Soc. of Agron., Inc., Madison, Wisc., 1986.

Nkeddi-Kizza, P., P. S. C. Rao, and A. G. Hornsby, Influence of organic cosolvents on leaching of hydrophobic organic chemicals through soils, *Environ. Sci. Technol.*, *21*(11), 1107–1111, 1987.

Oliver, B. G., Desorption of chlorinated hydrocarbons from spiked and anthropogenically contaminated sediments, *Chemosphere*, *14*(8), 1087–1106, 1985.

Parker, J. C., and M. T. van Genuchten, Determining transport parameters from laboratory and field tracer experiments, *Bulletin 84-3, Virginia Agricultural Experiment Station, Blacksburg*, Virginia Polytech. Inst. and State Univ., Blacksburg, Va., 1984.

Partyka, S., S. Zaini, M. Lindheimer, and B. Brun, The adsorption of non-ionic surfactants on a silica gel, *Colloids and Surfaces*, *12*, 255–270, 1984.

Pennell, K. D., L. M. Abriola, W. J. Weber Jr., Surfactant-enhanced solubilization of residual dodecane in soil columns, 1, Experimental investigations, *Environ. Sci. Technol.*, *27*(12), 2332–2340, 1993.

Press, W. H., S. A. Teukolsky, W. T. Vetterling, and B. P. Flannery, *Numerical Recipes in FORTRAN, The Art of Scientific Computing*, Cambridge University Press, New York, 1992.

Prickett, T. A., T. G. Naymik, and C. G. Lounquist, A "random-walk" solute transport model for selected groundwater quality evaluations, *Ill. State Water Surv., Champaign, Bull.*, *65*, 1981.

Ramila, P. B. S., Quantification of interactions between inhibitory primary and secondary substrates, Ph.D. thesis, *Univ. of Illinois at Urbana-Champaign*, Urbana, 1990.

Robson, R. J., and E. A. Dennis, The size, shape, and hydration of nonionic surfactant micelles, Triton X-100, *J. Phys. Chem.*, *81*(11), 1075–1078, 1977.

Schulz, H. D., and E. J. Reardon, A combined mixing cell/analytical model to describe two-dimensional reactive solute transport for unidirectional groundwater flow, *Water Resour. Res.*, *19*(2), 493–502, 1983.

Seinfeld, J. H., and L. Lapidus, *Mathematical Methods in Chemical Engineering, vol. 3, Process Modeling, Estimation, and Identification*, Prentice Hall, Englewood Cliffs, NJ, 1974.

Shiu, W. Y., and D. Mackay, A critical review of aqueous solubilities, vapor pressures, Henry's law constants, and octanol-water partition coefficients of the polychlorinated biphenyls, *J. Phys. Chem. Ref. Data*, *15*(2), 911–929, 1986.

Šimůnek, J., and D. L. Suarez, Two-dimensional transport model for variably saturated porous media with major ion chemistry, *Water Resour. Res.*, *30*(4), 1115–1133, 1994.

Somasundaran, P., E. D. Snell, and Q. Xu, Adsorption behavior of alkylarylethoxylated alcohols on silica, *J. Colloid and Interface Sci.*, *114*(1), 165–173, 1991.

Srinivasan, P., and J. W. Mercer, Simulation of biodegradation and sorption processes in ground water, *Ground Water*, *26*(4), 475–487, 1988.

Valsaraj, K. T., and L. J. Thibodeaux, Relationships between micelle-water and octanol-water partition constants for hydrophobic organics of environmental interest, *Water Res.*, *23*(2), 183–189, 1989.

van Genuchten, M. T., and W. J. Alves, Analytical solutions of the one-dimensional convective-dispersive solute transport equation, USDA, *Tech. Bull. 1661*, U.S. Dep. of Agric., Washington, D. C., 1982.

van Genuchten, M. T., and J. C. Parker, Boundary conditions for displacement experiments through short laboratory soil columns, *Soil Sci. Soc. Am. J.*, *48*, 703–708, 1984.

Wershaw, R. L., A new model for humic materials and their interactions with hydrophobic organic chemicals in soil-water or sediment-water systems, *J. Contam. Hydrol.*, *1*, 29–45, 1986.

Wilson, J. T., E. G. Enfield, W. J. Dunlap, R. L. Cosby, D. A. Foster, and L. B. Baskin, Transport and fate of selected organic pollutants in a sandy soil, *J. Environ. Qual.*, *10*, 501–506, 1981.

Z. Adeel and R. G. Luthy, Department of Civil and Environmental Engineering, Carnegie Mellon University, Pittsburgh, PA 15213. (e-mail: za22@andrew.cmu.edu;Luthy@cmu.edu)

D. A. Edwards, H & A of New York, 189 North Water Street, Rochester, NY 14604.

(Received October 28, 1994; revised April 17, 1995;
accepted April 24, 1995.)